

THE HIGH-TEMPERATURE PROPERTIES OF WELDED CAST CO-BASE ALLOYS

Dr. T. F. Chase and A. M. Beltran

General Electric, Materials and Processes Laboratory, Schenectady, New York

Abstract

The weldability of contemporary cast Co-base superalloys used in gas turbine vane applications is reviewed. Weldments were produced in two different strength-level alloys, FSX-414 and MM-509, using the Gas-Tungsten-Arc (GTA) and Electron Beam (EB) processes. Hot-cracking tendencies were evaluated as a function of filler alloy for GTA weldments. The response to post-weld solution treatment was measured by transverse-weld tensile and stress-rupture tests. Weldments were also subjected to service-simulated oxidation and hot-corrosion atmospheres in a small combustion burner rig. Fluidized-bed thermal fatigue testing was conducted on weldments utilizing Glenny-type tapered discs. Crack initiation and propagation data were obtained on smooth and notched configurations, respectively.

Introduction

Weld repair and joining techniques are essential elements in the manufacture and overhaul of gas turbine nozzle guide vanes. Repair of casting defects, such as hot tears and shrinkage porosity, repair of service-generated thermal-fatigue cracks, and the joining of nozzle assemblies, are the main areas of concern. The manual Gas-Tungsten-Arc (GTA) and Electron Beam (EB) welding techniques are most commonly utilized, yet little is actually understood of weldment properties or the behavior of weldments in service.

The principal problem associated with welding superalloys is their pronounced hot-cracking sensitivity. Highly-segregated, high-strength cast Co-base nozzle alloys are especially prone to hot cracking (Figure 1). While alloy composition and microstructure are certainly important factors, nozzle geometry and residual casting stresses also strongly influence weldability. It is important, therefore, that welding alloys and procedures be optimized in order to reduce the severity of hot cracking.

This paper presents the results of work in-progress being conducted on two representative Co-base vane alloys, FSX-414 and MM-509 (Table 1). FSX-414, developed by General Electric(1), is a modest rupture-strength alloy with excellent oxidation and hot-corrosion resistance. It features a higher-chromium and lower-carbon content than the familiar alloy X-40, and is strengthened primarily by the precipitation of Cr_{23}C_6 . MM-509, developed by Martin Metals(2), is the strongest cast Co-base alloy commercially available, due to a higher carbon content and the precipitation of Cr_{23}C_6 and TaC. MM-509 is generally used in the as-cast condition, while FSX-414 is given a two-step heat treatment (2100°F/4 hrs. + 1800°F/4 hrs.).

TABLE 1
BASE AND FILLER ALLOY COMPOSITIONS (WT. %)

<u>Alloy</u>	<u>Co</u>	<u>Ni</u>	<u>Cr</u>	<u>W</u>	<u>Ta</u>	<u>Zr</u>	<u>Fe</u>	<u>Si</u>	<u>Mn</u>	<u>C</u>
FSX-414	Bal.	10	29	7	---	---	2 max.	1 max.	1 max.	0.25
FSX-414LC	Bal.	10	29	7	---	---	2 max.	1 max.	1 max.	0.1
MM-509	Bal.	10	23.5	7	3.5	0.5	2 max.	0.2 max.	0.2 max.	0.6
L-605	Bal.	10	20	15	---	---	3	1	---	0.1
MM-918	Bal.	20	20	---	7.5	---	---	---	---	0.05
Hastelloy X	1.5	Bal.	22	0.6	(9 Mo)	---	18	---	---	0.1

GTA Studies

Alloys

Commercial filler alloys L-605, Hastelloy X, and FSX-414 (regular and low carbon) were selected for weldability studies with FSX-414 (Table 1). The same alloys were evaluated with MM-509, except that Hastelloy X was replaced by MM-918. This latter alloy was originally developed by Martin Metals for high-temperature sheet applications similar to L-605. However, its chemical composition suggested a measure of compatibility with MM-509; hence, it was evaluated in weldments.

Wire electrode of these filler alloys was obtained as follows:

L-605 - Uncoated 1/8" diameter electrodes were procured from a commercial source in accordance with AMS specification 5796.

FSX-414 (regular and low carbon) - 3/16" diameter by 6" rods were investment cast from small remelt ingots and GTA-welded into longer lengths.

MM-918 - Initially, 1/16" thick sheets were sheared to approximately a square cross-section; later, 1/16" diameter rods were swaged from 1/4" diameter extruded bar stock.

Hastelloy X - 3/32" diameter by 2' drawn rods were procured from a commercial source to AMS specification 5798.

Thick section welds were prepared in investment cast weld plates (nominally 1" X 4" X 6") of FSX-414 and MM-509; tensile and rupture specimens were cut from these plates along with unwelded control specimens. Thermal-fatigue discs and 1" diameter corrosion disc bar stock were investment cast by Misco Division of Howmet Corporation.

Welding Parameters

GTA welding of investment cast Co-base alloys exhibiting a high heat-affected-zone (HAZ) hot-cracking sensitivity requires certain precautions. For instance, heat input and volume of molten metal should be minimized. Hence, the welding parameters typical of those employed in this investigation are:

Technique - manual GTA/cold wire
Base Material Condition - solution treated
Filler Metal Wire Size - as above
Welding Current - 60 to 80 amps
Welding Voltage - approximately 12 volts SPDC
Shielding - 15 cfh argon
Electrode - 1/16" diameter, 2% thoriated tungsten, ground to 90° conical tip

The following procedure was used to prepare mechanical test specimens from thick weld plates:

1. Machine 60° included-angle double-V weld prep for butt-welding of 3/4" thick plate.
2. Ultrasonically clean and vapor degrease.
3. Make root pass and air-cool to room temperature
4. Conduct alternate weld passes and dye check for cracks; grind out and re-weld, if necessary, to insure sound weld.
5. Re-solution heat treat prior to specimen machining, as required.

Filler Alloy Evaluation

Initially, studies were conducted to determine whether the hot-cracking sensitivity of FSX-414 and MM-509 could be minimized through proper filler alloy selection. In general, the filler alloy should melt at a lower temperature than the incipient melting point of the substrate and be free of liquid-metal embrittling segregates. In addition, the filler alloy should exhibit a slow strength recovery during solidification and cooling, have good high-temperature ductility, and be metallurgically compatible with the substrate. These desirable metallurgical characteristics coupled with alloy availability should form the guidelines for filler alloy selection.

In the case of MM-509, high-constraint welds were evaluated by machining deep grooves (1/2" wide at the top tapered to 1/8" at the bottom, 1/2" deep) into 3/4" thick weld plates (Figure 2). Both as-cast and solution-treated (prior to welding) conditions were evaluated. The grooves were then filled with the appropriate filler wire using identical parameters and procedures. Metallographic specimens were removed at various levels parallel to the top surface. This investigation clearly identified MM-918 as the filler alloy least likely to induce hot cracking, and also that solution treatment significantly reduces hot cracking.

Thin- and thick-section welds in FSX-414 demonstrated essentially equivalent behavior with Hastelloy X, L-605, and low-carbon FSX-414 filler alloys. However, regular-carbon FSX-414 filler produced severe hot cracking in the root pass during butt-welding. Consequently, this filler was eliminated from further consideration.

GTA Weldment Properties

Mechanical Properties of Welded MM-509 - Transverse weldments, produced with MM-918 filler, were tensile and rupture tested in both the as-cast and post-weld solution-treated condition (2250°F/4 hrs.). Tensile testing established that the

unwelded control specimens from the thick solution-treated weld plates have significantly lower yield and ultimate tensile strengths than standard cast-to-size (CTS) bars between room temperature and approximately 1400°F (not shown). The welded, as-cast bars gave results essentially equivalent to the control bars (Table 2, Figure 3). The post-weld solution treatment caused a slight reduction in yield strength and increase in ductility.

TABLE 2
GTA-WELDMENT TENSILE PROPERTIES
OF MM-509 WITH MM-918 FILLER

<u>Condition</u>	<u>Temp., °F</u>	<u>UTS, ksi</u>	<u>0.2% YS ksi</u>	<u>0.02% YS ksi</u>	<u>% El</u>	<u>% RA</u>
As-Welded	Room	70.7	----	56.6	1.7	24.6
	800	70.8	54.2	41.2	5.0	10.0
	1200	65.7	50.2	39.1	5.4	10.8
	1600	49.0	39.0	31.0	15.6	32.6
Post-Weld Solution-Treated (2250°F/4 hrs.)	Room	87.0	71.2	57.2	3.8	7.8
	800	72.5	46.2	35.0	7.4	13.8
	1200	65.0	42.2	33.5	8.4	13.2
	1600	54.2	36.8	27.6	14.9	27.2

However, all of the welded bars failed well outside of the fusion and HAZ, i.e. in base material. Therefore, the weldments do not appear to be limiting in tension.

Stress-rupture testing, designed for 100-hour lives at 40, 30, 20, and 10 KSI, was also conducted on as-cast and post-weld solution-treated material (Table 3).

TABLE 3
GTA-WELDMENT RUPTURE PROPERTIES
OF MM-509 WITH MM-918 FILLER

<u>Condition</u>	<u>Temp., °F</u>	<u>Stress, ksi</u>	<u>Life, Hrs.</u>	<u>% El</u>	<u>% RA</u>	<u>Pc=20</u>	<u>Fracture Location</u>
As-Welded	1430	40	113.9	11.4	41.0	42.4	Base
	1540	30	58.1	11.3	44.0	43.6	Base
	1680	20	43.1	11.6	50.0	46.4	Base
	1880	10	53.5	----	----	50.9	HAZ
Post-Weld Solution-Treated (2250°F/4 hrs.)	1430	40	19.9	5.8	36.0	40.3	HAZ
	1540	30	16.6	6.3	32.0	42.5	HAZ
	1680	20	12.9	2.2	50.0	45.2	HAZ
	1880	10	11.2	----	----	49.4	HAZ

The results are also plotted in Figure 4 versus the as-cast cast-to-size bar rupture scatterband. In the as-welded condition, three of the four specimens failed in base material, and the results fell short of the CTS bar scatterband. However, the 1880°F/10 KSI specimen fractured in the HAZ with a very short life. This suggests that the HAZ may become increasingly limiting with increasing temperature, i.e. at higher parameters.

Post-weld solution treatment significantly reduced rupture strength, with the result that all four specimens failed in the HAZ with lower ductility (Figure 5). Lives were only one-fourth that of the as-welded specimens. It is significant, however, that none of the failures occurred through the nominally lower strength filler alloy, despite the fine substructure. It appears that the solutioning and aging occurring during the welding process, the subsequent solution treatment, and the aging that occurs during testing produce a carbide/matrix HAZ structure that is susceptible to brittle failure. Indeed, the weld fusion zone exhibited excellent ductility. Therefore, failure through the HAZ is caused by the effects of the welding process upon the base material and the subsequent thermal treatment and is not directly related to filler alloy chemistry or HAZ microfissuring.

Oxidation and Hot-Corrosion Resistance of FSX-414 Weldments - A very important criterion for weldments in critical gas-path locations is surface stability, or resistance to oxidizing or sulfidizing atmospheres. Ideally the filler alloy should exhibit inherent resistance equivalent to the base alloy. In addition, the HAZ and weldment substructures should also be immune to preferential attack.

The preferred means of assessing surface stability is the dynamic combustion burner rig; this is described in detail elsewhere(3). Two types of environments are of interest: (i) "normal" oxidation owing to the combustion of natural gas, and (ii) "hot corrosion" produced by the combustion of doped diesel oil (1% S) containing 475 ppm sea salt. At an air:fuel ratio of approximately 60:1 at 1600°F, this results in 8 ppm sea salt in the combustion products -- a severe, simulated-marine atmosphere.

GTA weldments were made in 1/8" radius grooves in a 1 1/8" diameter by 8" long FSX-414 bar with L-605, Hastelloy X, and FSX-414LC (low carbon) (Figure 6). Corrosion discs 1" O.D. by 1/16" thick were cut transverse to the weldments following a 2150°F/4-hour solution treatment and tested at 1600 and 1800°F in both environments. Attack was assessed on metallographically-prepared cross-sections at 100X as: (i) average bulk alloy surface loss, and (ii) maximum penetration. The latter may occur as oxide or sulfide attack along grain boundaries or interdendritic regions, or in weldments, as "spike" attack of segregated substructures.

In general, the data show the weldments are as resistant to oxidation and hot corrosion as FSX-414 base material (Table 4), with the possible exception of L-605 and FSX-414LC in 1800°F hot corrosion.

TABLE 4
SURFACE STABILITY OF GTA-WELDED FSX-414

<u>Material</u>	<u>Natural Gas</u>				<u>Diesel Oil + Sea Salt</u>			
	<u>1600°F/6057 Hrs.</u>	<u>1800°F/604 Hrs.</u>	<u>1600°F/600 Hrs.</u>	<u>1800°F/600 Hrs.</u>	<u>1600°F/600 Hrs.</u>	<u>1800°F/600 Hrs.</u>	<u>1600°F/600 Hrs.</u>	<u>1800°F/600 Hrs.</u>
	<u>M.P.(1)</u>	<u>S.L.(2)</u>	<u>M.P.</u>	<u>S.L.</u>	<u>M.P.</u>	<u>S.L.</u>	<u>M.P.</u>	<u>S.L.</u>
FSX-414 Base	4.2	0.3	3.5	0.3	4.2	0.4	5.3	0.3
FSX-414LC	5.1	0.6	24.7*	0.3	3.9	0.6	8.9	0.5
Hastelloy X	5.5	0.5	4.1	0.2	2.0	0.3	6.4	0.3
L-605	4.9	0.5	4.1	0.4	Not Tested		8.2	0.4

* Attack along a weld hot-crack.

(1) M.P. - Maximum Penetration, mils

(2) S.L. - Surface Loss, mils

However, behavior of the weldments was influenced to a large degree by orientation (Figure 7a) and the extent of carbide stringing. In most cases, preferential attack occurred along aligned carbides in the weld, at some acute angle to the specimen surface. Attack was negligible when alignment was parallel to the surface (Figure 7b). Previous studies(4) have shown that L-605, Hastelloy X, and FSX-414 have good surface stability between 1600 and 1800°F. At higher temperatures, FSX-414 and Hastelloy X are superior to L-605. This work, however, suggests that weldment structure and orientation may be equally as important as bulk alloy composition.

Thermal-Fatigue Resistance of GTA-Welded FSX-414 - Thermal-fatigue behavior is another important criterion for vane airfoil trailing edges. Two major considerations in this area are: (i) weld repair of service-generated thermal-fatigue cracks, and (ii) behavior of the weldment itself in a cyclic thermal environment.

To evaluate the thermal-fatigue behavior of weldments, investment cast FSX-414 Glenny discs(5) were procured (Figure 8). The discs were machined (three 3/8" wide by 1/2" deep slots, 120° apart), solution treated at 2100°F for four hours, GTA-welded with the above filler alloys, resolutioned plus aged at 1800°F for four hours, and final machined. Testing was conducted on unnotched specimens in fluidized beds, as follows:

1. Immersed in hot bath (1688°F for 4 minutes).
2. Transferred to cold bath (transfer time ~ 3.5 seconds).
3. Immersed in cold bath (75°F for 4 minutes).
4. Specimen optically examined at 54X every 5 cycles for crack initiation.

Crack initiation and growth data (after 50 cycles) were accumulated; these are listed in Table 5 (see next page) and graphically illustrated in Figure 9. Four different trailing edge radii were evaluated, since thermal stress and corresponding strain decreases with increasing radius. In all cases, the L-605 and FSX-414 (regular carbon) weldments were equivalent to each other but much less resistant to crack initiation than the FSX-414 base alloy. The weldments were also less resistant to crack propagation; however, L-605 was more resistant than FSX-414.

A number of factors appear to be responsible for the poor thermal-fatigue resistance of these weldments. For instance, grain growth during weld metal solidification is perpendicular to the instantaneous solid-liquid interface. Therefore, these weldments tend to consist of columnar grains, with grain boundaries aligned perpendicular to the surface. In addition, the partitioned solute composition is enriched in carbon, resulting in interdendritic and grain boundary stringer-like carbides which act as crack propagation paths (Figure 10).

An additional problem with FSX-414 (regular carbon) filler is related to the use of cast electrodes. These weldments contained inclusions and porosity directly attributable to the lower quality air-melted electrodes. A potential remedy, therefore, is to prepare vacuum-melted stock suitable for extrusion, drawing, or swaging.

Electron Beam Welding Studies

Considerable interest has arisen in the fabrication of vane subassemblies by EB-welding. In most cases filler alloys are not required, which simplifies the metallurgical evaluation of interactions between the weldment and base alloy. The highly-concentrated EB heat source produces a smaller molten volume, less shrinkage, and a narrower HAZ than GTA. For example, the following typical parameters were used:

TABLE 5

Thermal Fatigue Resistance of GTA-Welded FSX-414

Peripheral Radius (In.)	After 50 Cycles								
	Cycles to Crack		No. of Cracks		Longest Crack (In.)		Total Crack Length (In.)		
	FSX-414*	L-605*	FSX-414	L-605	FSX-414	L-605	FSX-414	L-605	Base Material
0.010	< 5	< 5	2	4	0.094	0.095	0.182	0.171	0.036
0.010	< 5	< 5	2	1	0.082	0.185	0.112	0.185	
0.010	< 5	< 5	5	4	0.055	0.080	0.196	0.156	
0.020	< 5	< 5	2	3	0.170	0.054	0.285	0.089	0.033
0.020	15	< 5	4	2	0.035	0.064	0.120	0.081	
0.020	< 5	10	2	2	0.405	0.060	0.505	0.096	
0.030	50	>50	2	0	0.035	0	0.050	0	0.021
0.030	15	15	1	1	0.330	0.032	0.330	0.032	
0.030	20	41	2	0	0.010	0.015	0.010	0.015	
0.040	10	< 5	1	1	0.012	0.014	0.012	0.014	0.020
0.040	< 5	20	2	2	0.095	0.018	0.117	0.031	
0.040	41	25	2	1	0.035	0.060	0.045	0.060	

* Filler alloys; unnotched.

R-7

Voltage - 140 KV
 Beam Current - 8 to 10 ma
 Beam Deflection - 600 cps
 Chamber Pressure - 5×10^{-1} microns Hg
 Gun Angle - Vertical
 Work Angle - Horizontal
 Work Speed - 10 to 16 in./min.
 Gun to Work Piece Distance - 4.5 to 5.5"

Mechanical Properties of EB-Welded MM-509

Autogenous EB-welds were made in 1" thick solution-treated MM-509 cast slabs. Transverse tensile specimens were machined and tested with the results listed in Table 6 and plotted in Figure 11.

TABLE 6

MM-509 EB-Weldment Tensile Properties

<u>Condition</u>	<u>Temp., °F</u>	<u>UTS, ksi</u>	<u>0.2% YS ksi</u>	<u>0.02% YS ksi</u>	<u>% El</u>	<u>% RA</u>
As-Welded	Room	84.4	65.2	57.3	1.6	5.0
	800	68.1	46.6	37.5	4.7	9.6
	1200	64.6	50.2	41.75	4.1	5.7
	1600	46.2	37.6	31.1	15.5	23.7
Post-Weld Solution-Treated (2250°F/4 hrs.)	Room	91.2	69.0	56.0	4.0	8.0
	800	68.9	45.3	35.8	8.4	14.5
	1200	67.2	39.7	33.3	8.5	11.6
	1600	55.3	41.7	33.8	12.1	27.9

All of the as-welded and solution-treated specimens failed outside of the fusion and heat-affected zones; hence, the properties once again reflect base material. In fact, these data are consistent with the GTA results reported earlier. That is, large grain-size base material is lower strength than CTS bar material; and solution treatment reduces yield strength slightly and increases ductility.

Stress-rupture results (Table 7; Figure 12) show the post-weld solution-treated condition stronger than the as-welded material. All of the as-welded bars broke in base material, while the solution-treated bars failed in the HAZ with lower-rupture ductility. This is the reverse of the GTA results, where lower strengths were obtained in HAZ-fractured solution-treated material.

Thermal-Fatigue Behavior of EB-Welded FSX-414

Glenny specimens were machined from EB-welded FSX-414 discs and fully heat treated. As before, crack initiation studies were conducted in the same fluidized bed cycle on unnotched specimens with four different TE radii (Table 8). The results show a degradation of crack initiation resistance in the weld relative to the base alloy, but less than half the losses encountered in GTA-filler welds.

TABLE 7

MM-509 EB-Weldment Rupture Properties

<u>Condition</u>	<u>Temp., °F</u>	<u>Stress, ksi</u>	<u>Life, Hrs.</u>	<u>% El</u>	<u>% RA</u>	<u>Pc=20</u>	<u>Fracture Location</u>
As-Welded	1430	40	92.4	11.5	17.0	41.6	Base
	1540	30	55.1	11.3	57.0	43.5	Base
	1880	10	117.2	15.9	38.0	51.6	Base
Post-Weld Solution-Treated (2250°F/4 hrs.)	1430	40	405.9	5.3	8.5	42.8	HAZ
	1540	30	125.3	11.3	12.0	44.1	HAZ
	1880	10	134.3	8.1	15.0	51.8	HAZ

TABLE 8

Thermal-Fatigue Resistance of EB-Welded FSX-414

<u>Peripheral Radius, In.</u>	<u>Crack Initiation</u>		<u>Crack Propagation After 50 Cycles</u>	
	<u>Avg. Cycles to Crack (Smooth)</u>		<u>Avg. Crack Length, In. (Notched)</u>	
	<u>Base</u>	<u>Weld</u>	<u>Base</u>	<u>Weld</u>
0.010	49	41	0.020	0.098
0.020	71	43	0.024	0.110
0.030	111	63	0.020	0.066
0.040	116	82	0.008	0.060

Crack propagation data after 50 cycles were obtained on discs notched in the weld. Propagation rates were 3 to 7 times faster than notched base material. The average crack length in the weldments, however, was intermediate to the unnotched L-605 and FSX-414 filler data in the GTA studies. Metallographic studies showed that grain and substructure orientation once again control crack initiation and propagation behavior. Unlike GTA weldments, the primary dendrites and grain boundaries are essentially parallel to the surface. This accounts for the somewhat better crack initiation resistance of EB-welds. However, EB-welding generates a segregate-rich centerline containing excess carbon, which is an easy fracture propagation path once a crack has been initiated (Figure 13).

Discussion

The fundamental mechanisms of hot cracking are not fully understood, but it is generally accepted that both metallurgical and mechanical factors are involved. Hot cracking will occur if the following conditions exist: (i) within a critical, high-temperature range, a low-melting point phase or microconstituent exhibits limited plastic strain capability, plus (ii) the superimposed thermal stresses due to welding induce strains exceeding the limits of (i).

The steep temperature gradients and comparatively rapid temperature changes associated with welding produce unavoidable shrinkage stresses. Although shrinkage stresses

can be minimized by judicious selection of welding processes and parameters, elimination of the mechanical factors contributing to hot cracking is impossible. Consequently, consistent control of hot cracking is best achieved through the metallurgical factors.

This investigation has shown that hot cracking is primarily associated with carbide precipitates in FSX-414 and MM-509. Both alloys contain the pseudo-eutectic $M_{23}C_6$ carbide, which undergoes remelting in the fusion zone during welding. Resolidification, plus diffusion, nucleation, and growth of the carbide, produce a higher surface area-to-volume ratio morphology in the HAZ, which enhances brittle crack propagation.

The "Chinese"-script, Ta-rich MC carbide in MM-509 plays little or no role in weld hot cracking per se. Other studies(6) have demonstrated that it is stable virtually to the melting point of MM-509. However, it undoubtedly contributes to crack propagation under, for example, thermal-fatigue conditions. Since it does not solution, post-weld heat treatments are ineffective in terms of altering MC morphology or distribution.

It has also been shown that grain and substructure orientation of the weldment strongly influences both hot cracking and weldment properties such as thermal-fatigue resistance and surface stability. EB-welding appears to be superior to GTA in this regard, since less sensitive orientations and less segregation are produced. The reason for this is that EB-welding produces a tear-drop shaped weld puddle due to the comparatively high travel speed and sharp temperature gradient. Solidification occurs by epitaxial nucleation off the partially-melted HAZ grains; and growth proceeds normal to the solid-liquid interface(7). Therefore, the fusion zone grain boundaries are oriented essentially perpendicular to the fusion line. The major weakness of EB-weldments, however, is a solute-rich centerline grain boundary due to the impingement of the columnar grains along the puddle's trailing edge.

On the other hand, GTA weldments generally involve an elliptically-shaped trailing solid-liquid interface, thereby allowing a greater number of grains to survive during the competitive growth process. The resulting grain and substructure boundaries tend to be perpendicular to the surface. Along with the orientation effects, greater segregation occurs due to the shallower temperature gradients and slower growth rate.

To preserve adequate thermal-fatigue resistance in weld-repaired vanes, therefore, it appears that welding technique should be controlled to minimize such structures. For example, techniques such as pulsed arc would tend to break up the orientation effects normally found in GTA weldments.

Improper selection of filler alloy can also have a significant impact on thermal-fatigue resistance, particularly crack propagation resistance. Since the precipitation of stringer-like carbides at grain boundaries is detrimental, it is important that C content of the filler alloy be minimized. Carbon and other element levels may increase in the weldment by melting and mixing with the higher-carbon level base material and by diffusion from the HAZ. The increase in C level and the fine substructure in the fusion zone may also explain the lack of tensile or rupture failures in the GTA weldments. It is important to note that, as base materials, both MM-918 and L-605 are significantly weaker than MM-509 in stress rupture. Thus, the degradation in stress-rupture properties is due to the effect of the welding process on the HAZ and not the filler alloy.

The response of both GTA and EB weldments to heat treatment is also of interest. Initial studies of hot-cracking sensitivity demonstrated that solution treatment prior to welding significantly reduces this tendency. However, the response of $M_{23}C_6$ to the

2250°F/4-hour solution treatment is a function of carbide and grain size resulting from the solidification parameters associated with large parts. In highly-segregated castings, such as the thick weld plates used in this investigation, the large primary particles and eutectic colonies of $M_{23}C_6$ only partially solution; hence, the full benefit of the treatment may not have been realized.

Post-weld solution treatment of MM-509 appears to be of some benefit for EB weldments, in that the fine carbide network and substructure are solutioned. Aging during service eventually reverses this condition, as demonstrated by the rupture testing in this study. The narrower HAZ apparently prevents the degradation of strength, causing a reversal in ranking compared to as-welded versus solution-treated GTA welds. The latter apparently overaged during the exposure, causing early failure through the HAZ.

Summary

Weldment properties do not appear to be limited in tension, in that all welded specimens failed well outside of the fusion and heat-affected zones. However, weldment properties appear to be stress-rupture limiting in the post-weld solution-treated condition, since these specimens failed in the HAZ. Therefore, the weldments themselves exhibit superior strength; and degradation occurs in the base material adjacent to the fusion zone where overaging occurs.

This investigation also points out the importance of carbon level and orientation effects in the fusion zone. Stringer-like carbides oriented normal to the surface appear to lower the oxidation, hot-corrosion, and thermal-fatigue resistance of the fusion zone. The lower carbon level filler alloys are less prone to induce HAZ hot cracking, which is the major problem associated with welding investment-cast cobalt-base alloys. In general, EB-welding produces less property degradation than GTA due to the narrower HAZ.

References

- (1) A. D. Foster and C. T. Sims, Metal Progress, July 1969, p. 83.
- (2) H. L. Wheaton, Cobalt, No. 29, December 1965, pp. 163-70.
- (3) B. O. Buckland, A. D. Foster, and J. J. Treanor, NACE Conference, April 21, 1966, Miami, Florida.
- (4) H. V. Doering, Private Communication.
- (5) E. Glenny and T. A. Taylor, J. Inst. of Metals, 88, No. 11, 1960, pp. 449-461.
- (6) A. M. Beltran, C. T. Sims, and N. T. Wagenheim, J. Metals, September 1969, pp. 39-47.
- (7) W. F. Savage, C. D. Lundin, and T. F. Chase, Welding Journal, November 1968, pp. 522-S to 526-S.

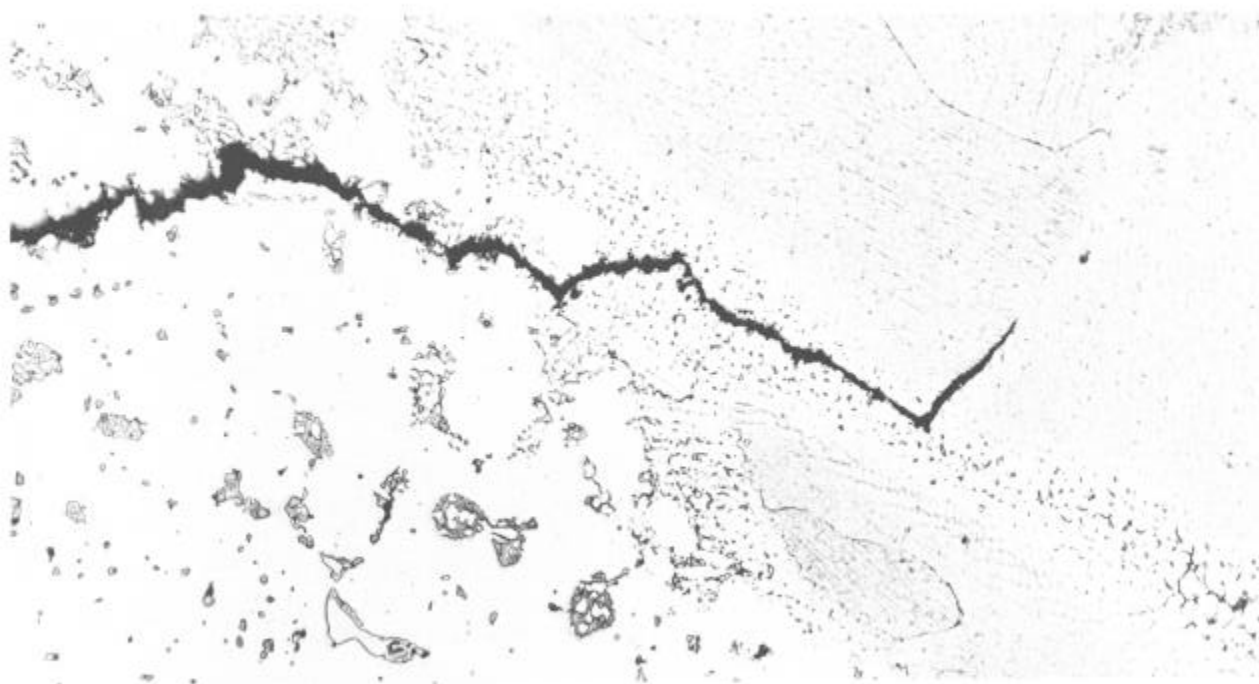


Figure 1. HAZ Hot Cracking of a Co-Base Superalloy. (200X)

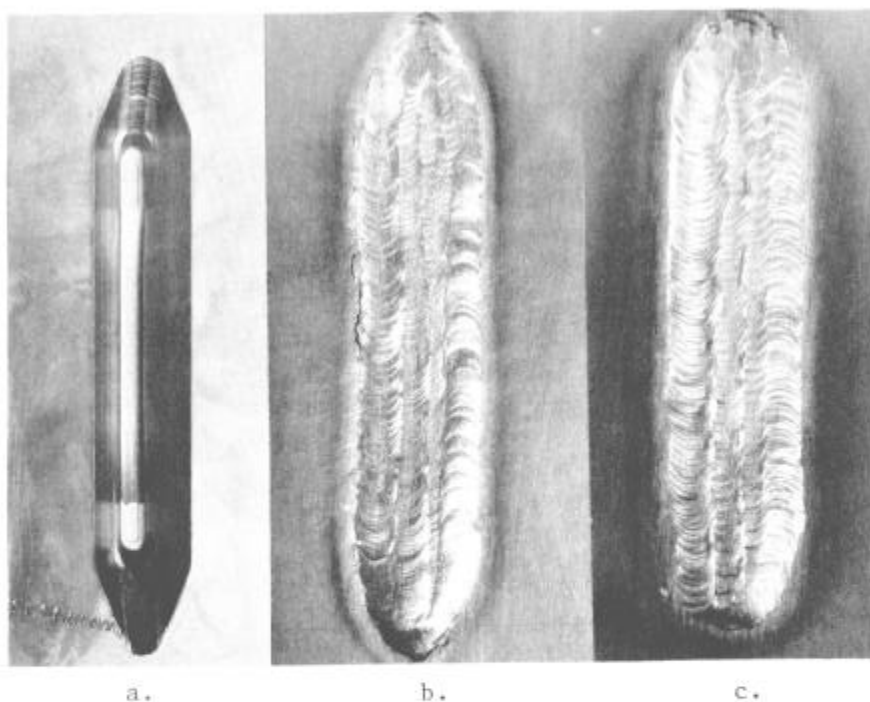


Figure 2. Deep-Groove GTA Weldment in MM-509. (1X)

- a. As-Machined Groove
- b. FSX-414LC Filler
- c. MM-918 Filler

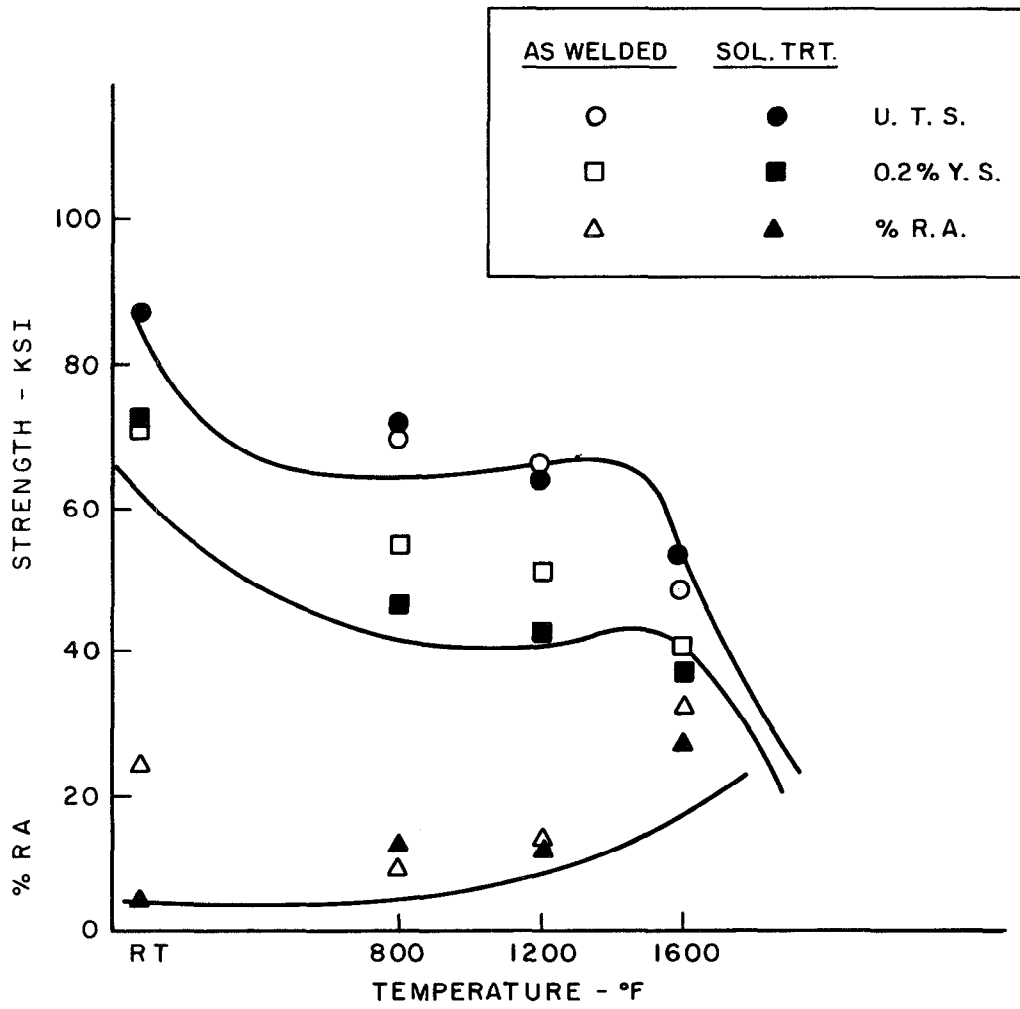


Figure 3. Tensile Properties of MM-509, GTA-Welded with MM-918 Filler.

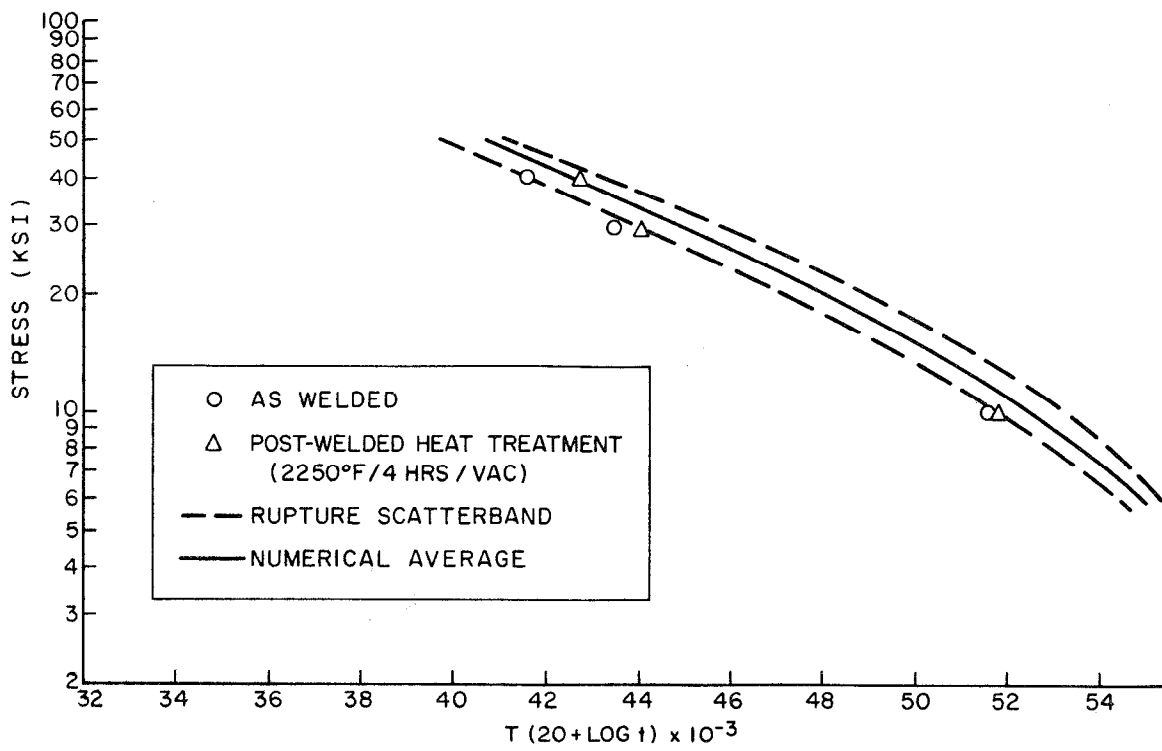


Figure 4. Stress-Rupture Properties of MM-509, GTA-Welded with MM-918 Filler.

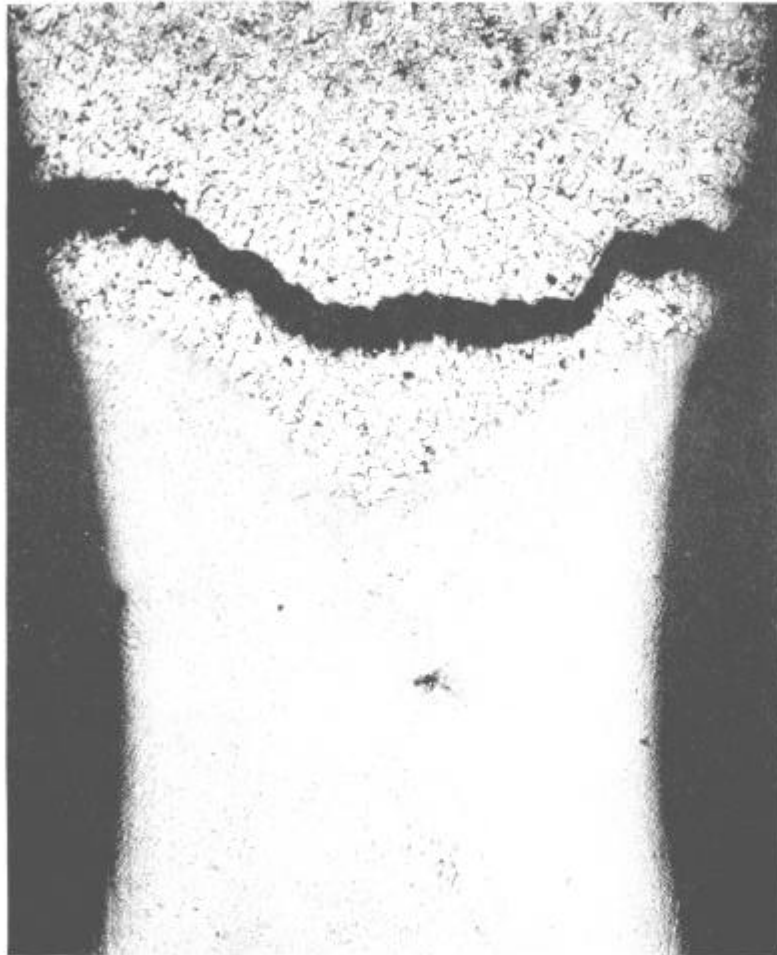
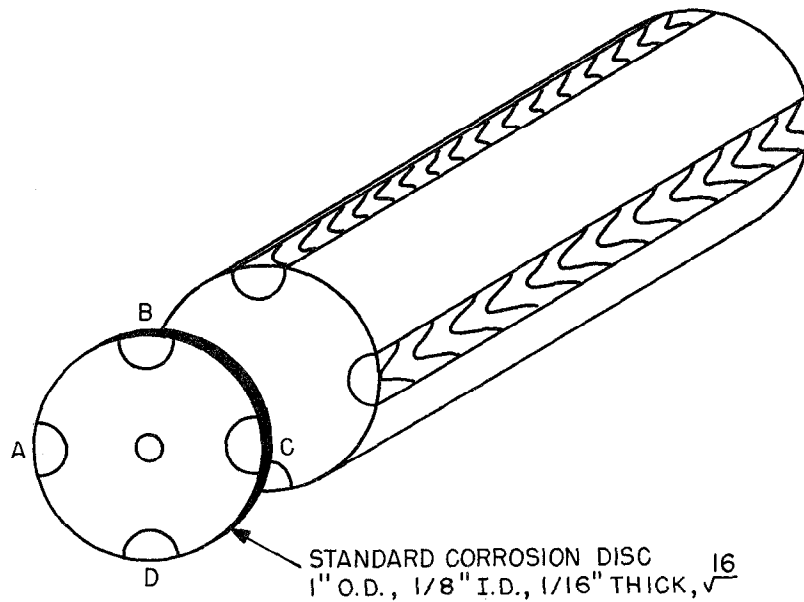
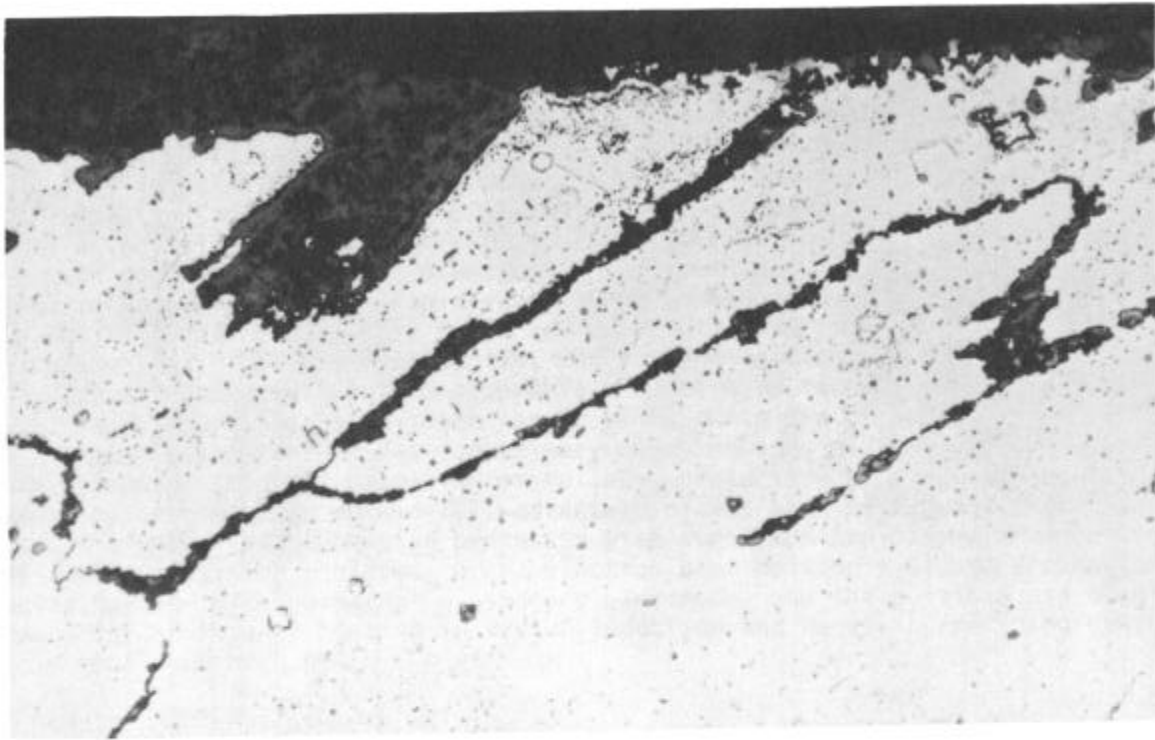


Figure 5. HAZ Failure in Post-Weld Solution-Treated Rupture Specimen; MM-509 with MM-918 Filler. (25X)

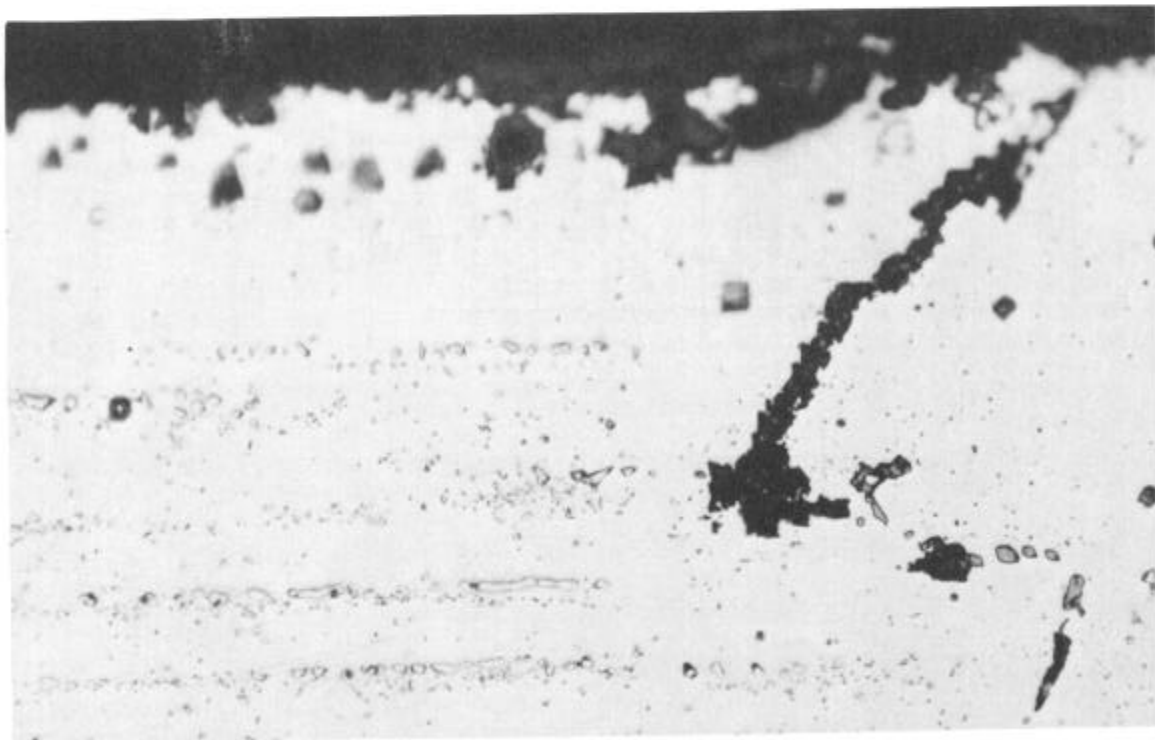


FILLER METAL KEY	
A	- EXPERIMENTAL ALLOY
B	- HAST X
C	- L-605
D	- FSX-414 LC

Figure 6. Test Bar and Specimen for Rig Testing of GTA Weldments.



a. Intersect Surface



b. Parallel to Surface

Figure 7. Orientation Effect of GTA Weldment on Oxidation Resistance. (500X)

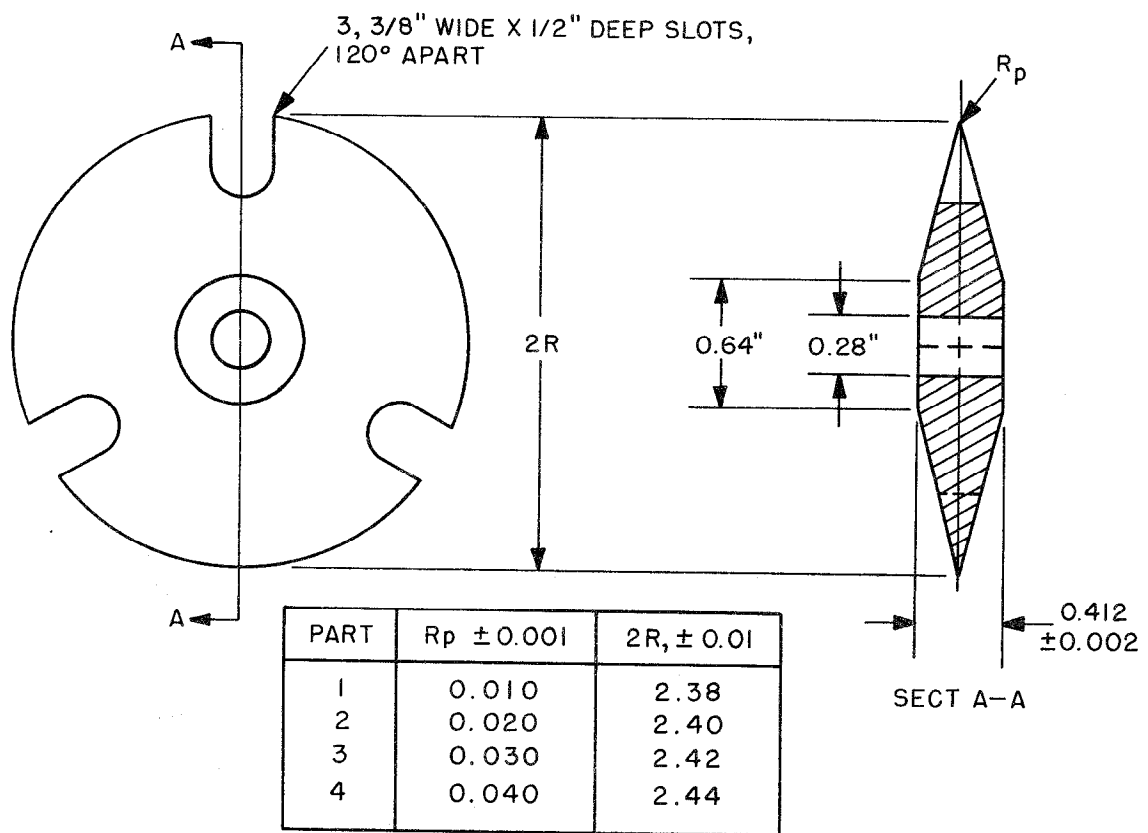


Figure 8. Glenny Specimen for Thermal-Fatigue Evaluation of GTA Weldments.

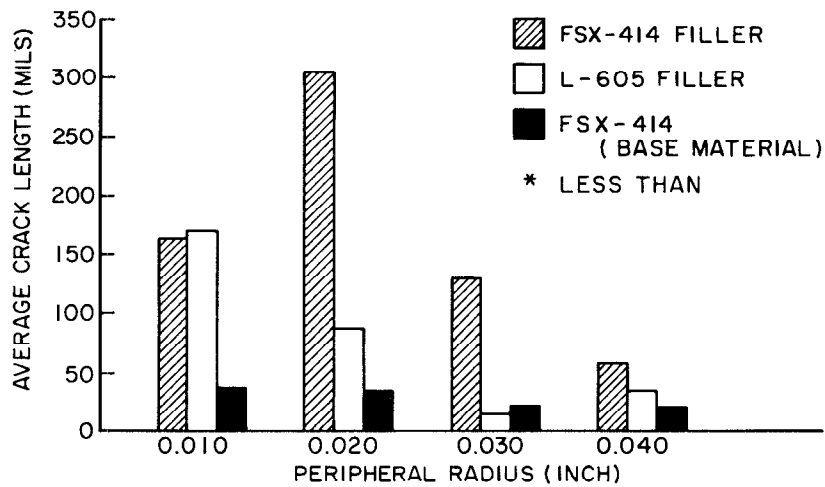
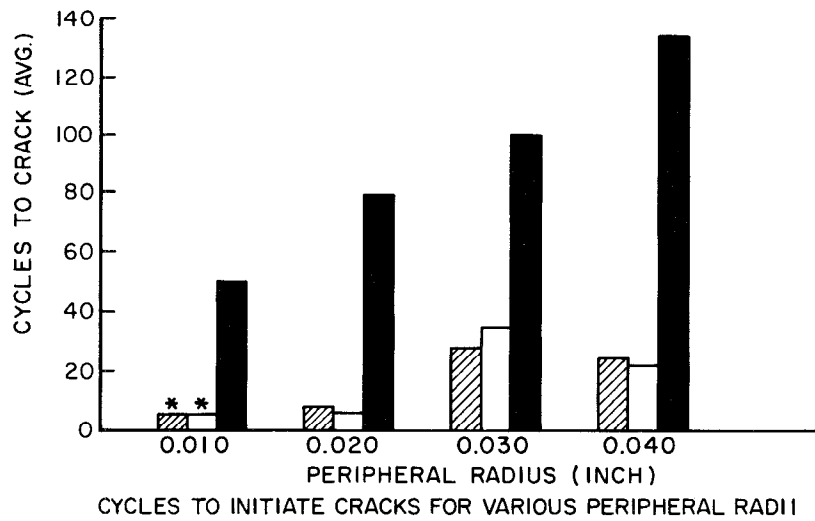


Figure 9. Thermal-Fatigue Crack Initiation and Growth Rates in GTA-Welded FSX-414.

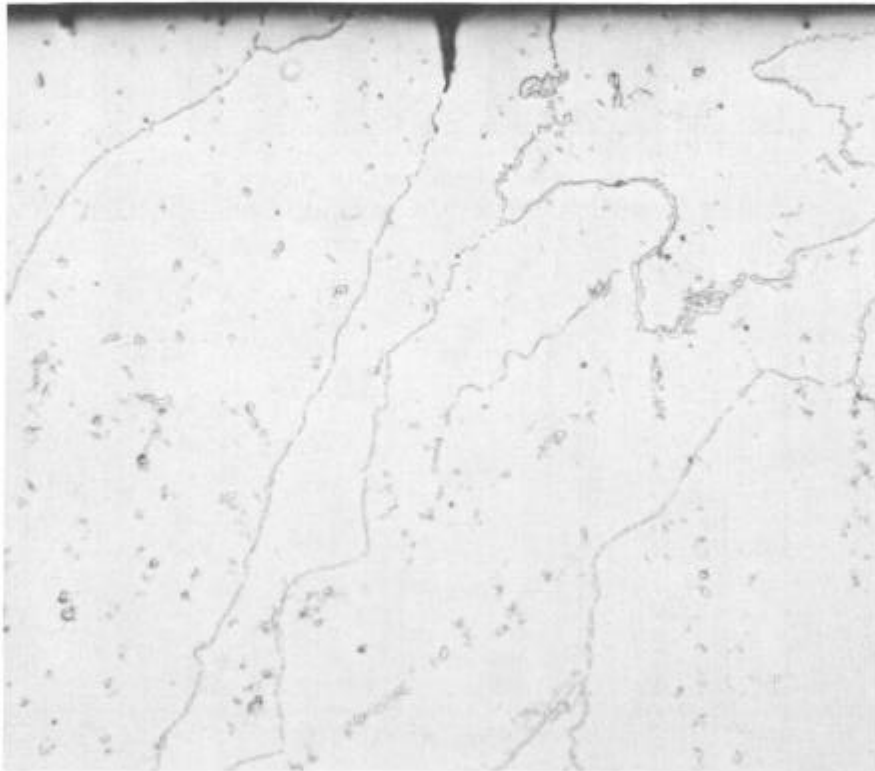


Figure 10. Thermal-Fatigue Crack Propagation Along Stringered Grain Boundary Carbides. (100X)

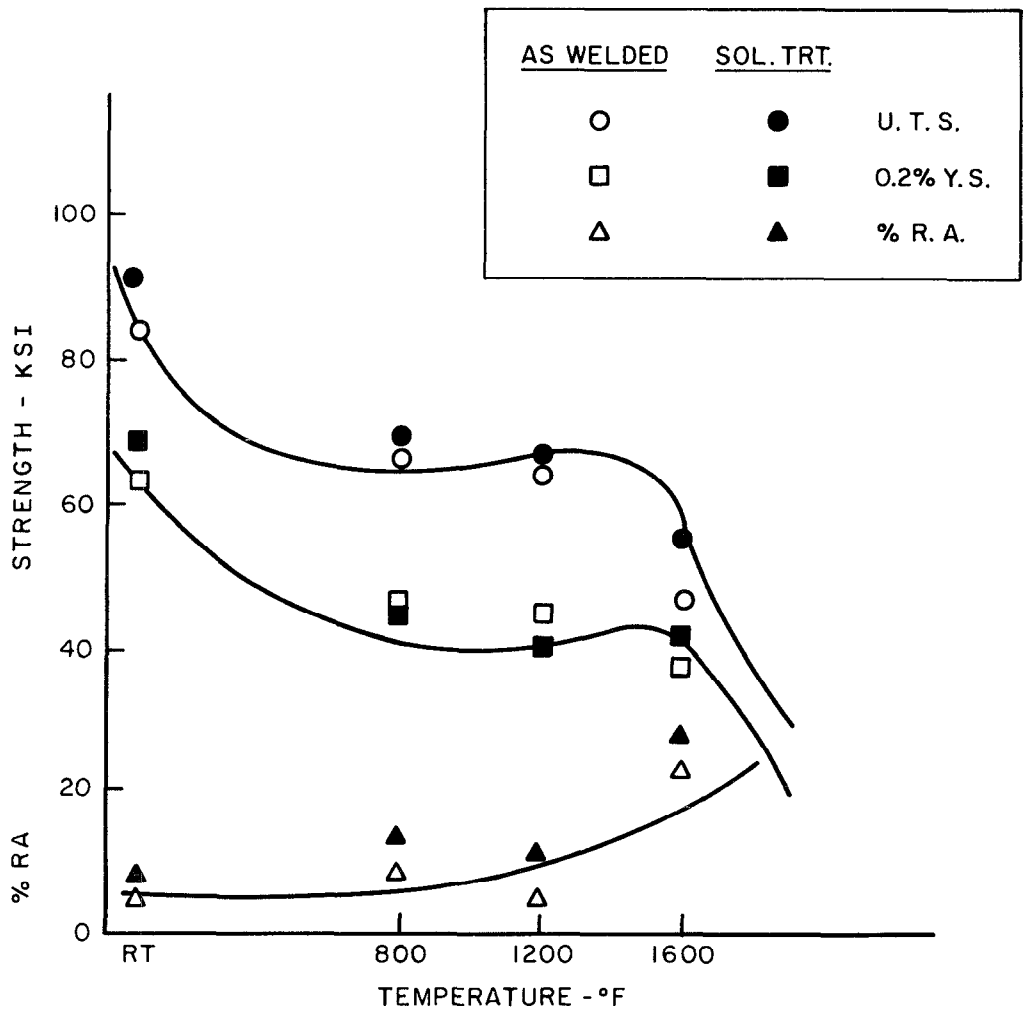


Figure 11. Tensile Properties of EB-Welded MM-509.

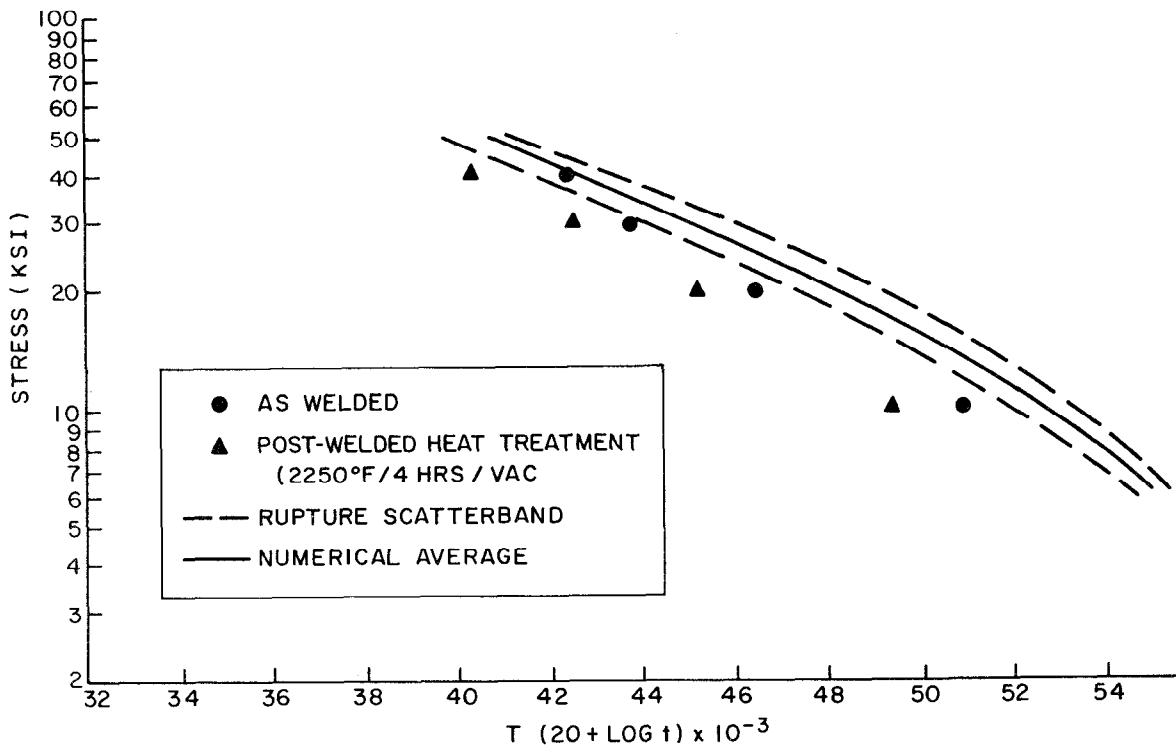


Figure 12. Stress-Rupture Properties of EB-Welded MM-509.

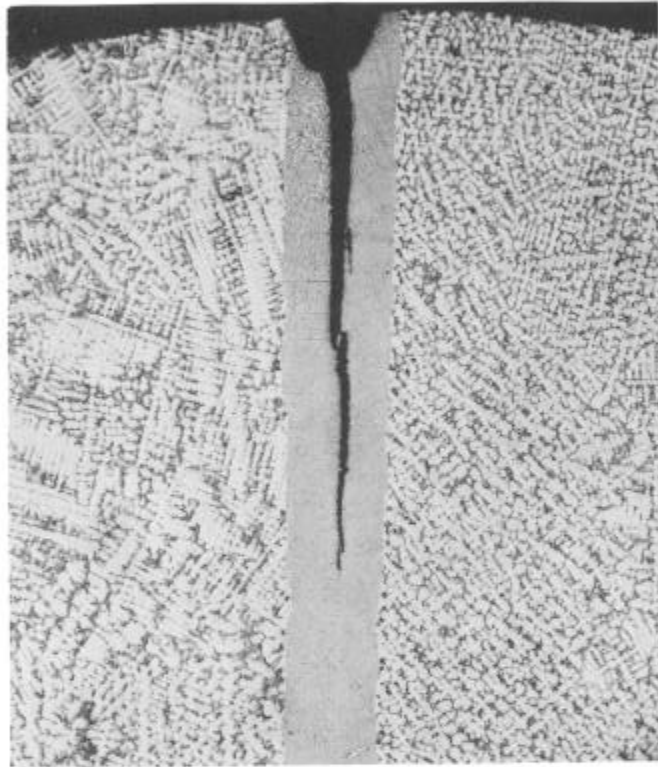


Figure 13. Thermal-Fatigue Crack Propagation Along EB-Weld Centerline at Notched Specimen. (10X)